Annealing effect on the reduction of Fermi-level density of states in CoTiSb: NMR evidence

C. S. Lue,[1,*] C. F. Chen,[1] Fu-Kuo Chiang,[2,3] and M.-W. Chu[2]

[1]*Department of Physics, National Cheng Kung University, Tainan 70101, Taiwan*
[2]*Center for Condensed Matter Sciences, National Taiwan University, Taipei 10601, Taiwan*
[3]*Department of Engineering and System Science, National Tsing Hua University, Hsinchu 300, Taiwan*

With the aim to examine the variation in the electronic properties of CoTiSb due to heat treatment, a comparative study of the as-cast and annealed samples using ^{59}Co nuclear magnetic resonance (NMR) spectroscopy was performed. All NMR observations clearly indicate a significant change in the local electronic characteristics for the annealed sample. The spin-lattice relaxation rate measurements further provide an estimate of Co-d Fermi-level density of states, $N_d(E_F)$, indicating a substantial reduction in $N_d(E_F)$ for the specimen with heat treatment. This finding gives a microscopic interpretation for the larger electrical resistivity and Seebeck coefficient in the annealed half-Heusler alloys, as the samples with higher electrical resistivity and Seebeck coefficient usually are associated with lower carrier densities in the vicinity of the Fermi level.

I. INTRODUCTION

Complex intermetallics have been of considerable interest in resent years because of their unconventional transport properties and magnetic behavior. One of the most intriguing systems is the ternary compounds of the general formula XYZ (X and Y are transition elements; Z=Sn or Sb) with the MgAgAs structure (space group $F\bar{4}3m$), frequently referred to as the half-Heusler compounds.[1–3] The materials of this type are derived from the cubic $L2_1$ Heusler phases X_2YZ by removing one of the equivalent X atoms, leaving a vacancy site. The half-Heusler systems are far from compact, and they can be stabilized only through covalent bonding within a restricted range of peripheral electron number. The ideal valence electron concentration (VEC) is 8 or 18 electrons per formula unit, which corresponds to MgAgAs, NiTiSn, CoTiSb, FeVSb, etc.[4–6] It leads to the formation of tetrahedral bonds and sp^3 hybridization around the p element and favors bonding between d metals.[7] Semiconducting and semimetallic behavior, indicated by the negative temperature coefficient of the electrical resistivity and a large Seebeck coefficient around room temperature,[4,5,8–12] are commonly observed in most half-Heusler compounds with VEC=18.[2–5,8,9]

Structural imperfection, particularly arising from site interchange, is likely to be an inherent feature in the half-Heusler family. As a consequence, the measured physical properties may considerably differ from sample to sample with different preparing and annealing processes.[10,13–15] There is general agreement from intense experimental results that heat treatment plays an important role for improving the structural perfection.[10,14,16,17] Observations of the enhancement in the thermal conductivity upon annealing had been attributed to the decrease in the grain-boundary and/or point-defect scattering.[10,14,17] Nevertheless, there has been little quantitative work associated with the local properties in these half-Heusler alloys, essential to interpret the variation in their electronic characteristics through heat treatment.

To gain microscopic insight into the changes in physical properties in the half-Heusler compounds via annealing, a comparative study of the as-cast and annealed CoTiSb samples using ^{59}Co nuclear magnetic resonance (NMR) spectroscopy was performed. NMR is known as an atomic probe yielding information about the Fermi surface features.[18] In this paper, we will present NMR measurements including line shapes, Knight shifts, and spin-lattice relaxation times in both as-cast and annealed CoTiSb compounds as related to their local electronic characteristics.

II. EXPERIMENTAL RESULTS AND DISCUSSION

Polycrystalline CoTiSb compounds were prepared from 99.95% Co, 99.9% Ti, and 99.999% Sb by mixing appropriate amounts of elemental metals, and were melted in an arc-melting furnace under a Zr-gettered argon atmosphere. Due to the volatility of Sb at high temperatures, we started with an excess of 3 mol % from stoichiometry for Sb. With the aim to examine the change in the electronic features via heat treatment, one part of the CoTiSb ingot remains no annealing while the other part was annealed in a vacuum-sealed quartz tube at 800 °C for two weeks and subsequently cooled with a rate of 60 °C/hr. X-ray diffraction (XRD) patterns of both powder specimens, shown in Fig. 1, were acquired on a Bruker D8 Advance diffractometer equipped with a monochromatic Cu $K\alpha$ radiation. Rietveld refinements of the powder patterns indicated that both samples crystallize in the MgAgAs-type structure ($F\bar{4}3m$) with a phase purity. The respective Rietveld-refined lattice parameters of the as-cast and annealed CoTiSb are of 5.8851 and 5.8832 Å, consistent with the previous reported values.[1,3,13,14] The chemical analyses of 20 crystals per specimen using energy-dispersive x-ray spectroscopy (EDS) in a transmission electron microscope (JEOL 2000FX, operated at 200 kV) further revealed the generally good control over the Sb stoichiometry, in agreement with the XRD refinements. The data from the structural and chemical analyses were tabulated in Table I. It is apparent that heat treatment has little effect on the Sb loss. In addition, a slight substoichiometry was found for Co and Ti in both specimens through the x-ray and chemical characterizations.
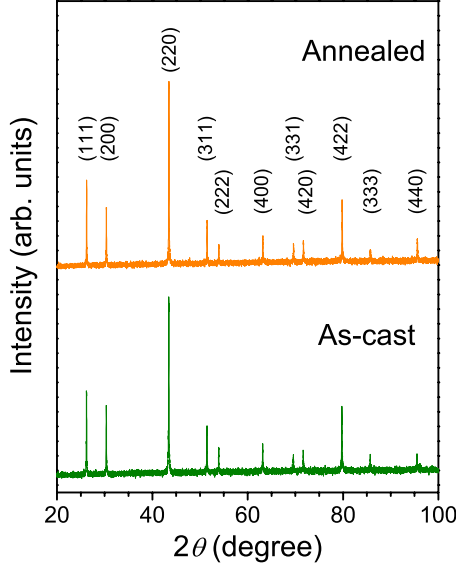
FIG. 1. (Color online) X-ray diffraction patterns for the as-cast and annealed CoTiSb. Reflections are indexed with respect to the MgAgAs-type structure.

FIG. 2. (Color online) Room-temperature ^{59}Co NMR powder patterns for the as-cast and annealed CoTiSb.

NMR measurements were performed using a Varian 300 spectrometer, with a constant field of 6.9437 T. A home-built probe was employed for both room-temperature and low-temperature experiments. Powder samples were used to avoid the skin depth problem of the rf transmission power. Each specimen was put in a plastic vial that showed no observable ^{59}Co NMR signal.[19] The Knight shifts here were referred to the ^{59}Co resonance frequency of one molar aqueous $K_3Co(CN)_3$.

A. Line shapes

In this investigation, ^{59}Co NMR line shapes of both Co-TiSb specimens were measured by spin-echo integration versus frequency. For the $F\bar{4}3m$ phase, there is a single Co site which is axially symmetric (asymmetry parameter $\eta = 0$). For the as-cast sample, the line shape appears as typical powder patterns, a strong central transition line ($m = -\frac{1}{2} \leftrightarrow +\frac{1}{2}$) with six distinctive satellite lines (indicated by arrows in Fig. 2).

In principle,[20] the first order quadrupole shift is the main effect shaping the satellite lines, and the quadrupole frequency ν_Q can be obtained directly from these lines as the separation of the adjacent lines equals to $\nu_Q/2$. The determined $\nu_Q \simeq 21$ kHz is rather small, suggesting that the Co site is located in a higher symmetric environment. For the annealed CoTiSb, the feature of these satellite lines is smeared out, attributed to the magnetically dipolar broadening from magnetic impurities. According to previous studies,[21,22] the annealed CoTiSb alloys contain more magnetic impurities that appear to be magnetic clusters and are responsible for the substantial enhancement in the magnetic susceptibility. To further identify this argument, we measured the magnetic susceptibility for both as-cast and annealed Co-TiSb, and showed the result in the inset of Fig. 3. As one can see, the susceptibility for the annealed sample is approximately an order of magnitude larger than the as-cast one, being consistent with the previous observations.[21,22]

NMR linewidths can provide a measure of the concentration of magnetic clusters in the vicinity of the NMR nucleus.[23–25] For the annealed CoTiSb, the resonance spec-

TABLE I. The atomic positions and the Rietveld-refined site occupations (n) and isotropic atomic displacement parameters (B_{iso}) of the as-cast and the annealed CoTiSb at room temperature using the space group $F\bar{4}3m$. The isotropic atomic displacement parameters of Co and Ti were constrained. EDS chemical analyses of the samples were also given. For each tabulated refined results, the first row is for the as-cast sample, while the second row is for the annealed one.

Atom	Wyckoff	x	y	z	B_{iso}	n	n (EDS)
Co	4c	1/4	1/4	1/4	1.18(9)	0.81(9)	0.80
					0.79(9)	0.84(9)	0.81
Ti	4b	1/2	1/2	1/2	1.18(9)	0.85(9)	0.87
					0.79(9)	0.87(9)	0.88
Sb	4a	0	0	0	0.95(9)	0.99(9)	1.00
					0.93(9)	0.97(9)	0.98
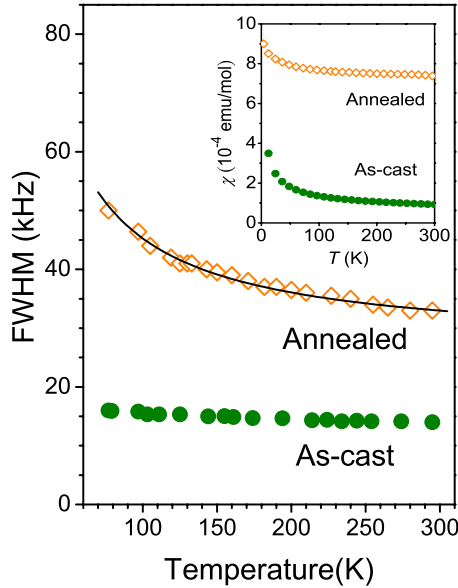
FIG. 3. (Color online) The variation of the ^{59}Co FWHM line-widths with temperature for the as-cast and annealed CoTiSb. The solid curve is a fit to the broadening for the annealed CoTiSb sample described in the text. Inset: the measured magnetic susceptibility for both as-cast and annealed CoTiSb.

trum exhibits a Lorentzian shape, as expected for broadening by dilute magnetic impurities.[24,25] As a measure of the line broadening, we recorded the full width at half maximum (FWHM) for different temperatures. While the NMR linewidth for the as-cast sample shows nearly temperature-independent, the FWHM for the annealed CoTiSb increases with decreasing temperature, following the Curie-type $1/T$ behavior as illustrated in Fig. 3. Walstedt and Walker have calculated the linewidth due to dilute magnetic impurities,[25] for the case where the fluctuation of the impurity spins is rapid compared with the NMR splittings, the line broadening is proportional to the average spin moment, giving a Curie-type contribution, as observed here. According to this theory, substitutional clusters having spin S and concentration c will produce a FWHM, $\Delta\nu$, which can be expressed as

$$\Delta\nu = \frac{2}{\ln 2}\frac{\gamma_n g \mu_B \mu_0 N c}{9\sqrt{3}R^3}|\langle S_z(T)\rangle|. \qquad (1)$$

Here, γ_n is the Co nuclear gyromagnetic ratio, μ_B is the Bohr magneton, and $\langle S_z(T)\rangle$ is the average moment of magnetic clusters. R and N represent the distance and the number of the nearest neighboring sites. In this fit, we fixed $g=2$ and $S=3/2$, assuming that the clusters contain the Co^{2+} moments. The least-squares fit, shown as a solid curve in Fig. 3, yields an impurity concentration $c=0.021$ for our annealed CoTiSb. In addition, the present NMR result indicates these magnetic clusters to be uniformly distributed within the sample. It is worthwhile mentioning that similar analyses have been applied to the Heusler compounds Fe_2VAl and Fe_2VGa.[26] The determined impurity concentrations have been found to be in good agreement with the observed up-turns in the low-temperature specific heat data.[27,28]
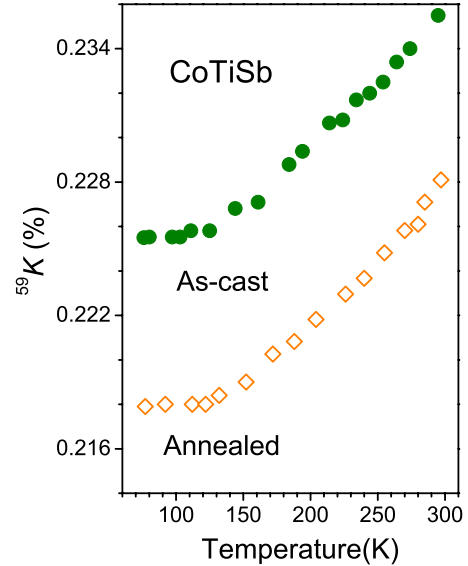
FIG. 4. (Color online) Temperature dependence of the ^{59}Co Knight shifts for the as-cast and annealed CoTiSb.

B. Knight shift

Figure 4 shows the temperature dependence of ^{59}Co NMR Knight shifts (^{59}K's) for the as-cast and annealed CoTiSb alloys. The values of ^{59}K for both materials were determined from the position of the maximum of each spectrum. Below 130 K, both ^{59}K's exhibit almost temperature independent. These constant terms mainly originate from the orbital (para-magnetic) shifts and thus are consistent with a small contact Knight shift contribution implied by the observed long T_1's. For the orbital shift, there is the general form[23]

$$K_{\text{orb}} = \frac{2e^2}{m^2c^2}\Sigma\frac{\langle\Psi|L_z|\Psi'\rangle\langle\Psi'|L_z/r^3|\Psi\rangle}{\Delta E} + \text{c.c.}, \qquad (2)$$

where Ψ is an occupied state, and the sum is over excited states Ψ'. ΔE represents the average band separation in the vicinity of the Fermi level. On this basis, the tiny ΔE in the denominator will cause a considerable orbital shift which can be used to explain the large ^{59}K's in both CoTiSb samples. Note that the magnitude of ^{59}K is reduced upon annealing, indicative of an increase in ΔE, being consistent with the result found in the spin-lattice relaxation rates at elevated temperatures.

Above 130 K, ^{59}K's shift to higher frequencies with rising temperature, reflecting an increase in the spin susceptibility, attributed to a thermally activated increase in the number of carriers, also responsible for the enhancement in the relaxation rate. Contrary to other gapped systems such as Fe_2VAl and Fe_2VGa,[29,30] the ^{51}V Knight shifts were found to shift to lower frequencies with increasing temperature, owing to the negative core polarization of vanadium d states. With this respect, we conclude that the thermally excited carriers in CoTiSb are mainly s-character, with positive s-hyperfine constant responsible for the T-dependent Knight shifts and spin-lattice relaxation rates at elevated temperatures. It is
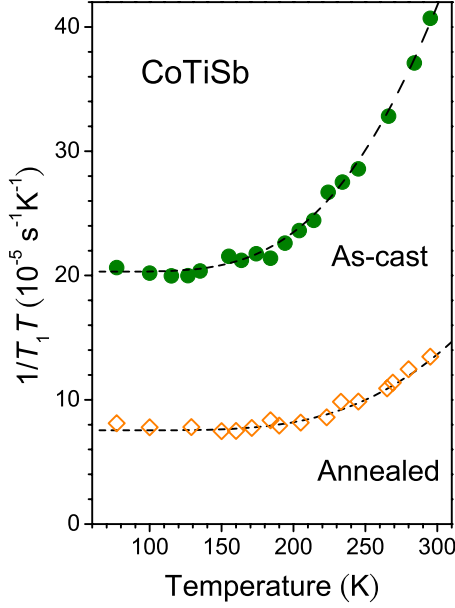
FIG. 5. (Color online) Temperature variation of $1/T_1T$ for the as-cast and annealed CoTiSb alloys. The dashed curves represent the fits to the semimetallic character from Eq. (5).

worthwhile mentioning that similar features have been observed in the semiconducting and semimetallic Co-based skutterudites.[19,31]

C. Spin-lattice relaxation rates

Temperature-dependence of the spin-lattice relaxation rate $(1/T_1)$ measurements were carried out using the inversion recovery method. We recorded the recovery of the signal strength by integrating the ^{59}Co spin-echo signal. In these experiments, the relaxation process involves the adjacent pairs of spin levels, and the corresponding spin-lattice relaxation is a multiexponential expression.[32] For the central transition with $I=7/2$, the recovery of the nuclear magnetization obeys

$$\frac{M(t) - M(\infty)}{M(\infty)} = -2\alpha(0.012e^{-t/T_1} + 0.068e^{-6t/T_1}$$
$$+ 0.206e^{-15t/T_1} + 0.714e^{-28t/T_1}). \quad (3)$$

Here, $M(t)$ is the magnetization at the recovery time t and $M(\infty)$ is the magnetization after long time recovery. The parameter α is a fractional value derived from the initial conditions used in our experiments. Each experimental T_1 was thus obtained by fitting to this multiexponential recovery curve.

As proposed by Moriya,[33] the mutual interaction of local moments can give a temperature-independent contribution in $1/T_1$. We, however, found no such effect in the annealed CoTiSb specimen. This suggests that those moments must be either quite small or distributed as clusters with low density, in agreement with the linewidth analysis. In Fig. 5, we show a plot of $1/T_1T$ versus temperature for the as-cast and annealed CoTiSb samples. Similar to the Knight shift results, the observed $1/T_1T$ can be separated by a constant term

$1/T_{1K}T$ and a thermally activated part. The $1/T_{1K}T$ term is the Korringa constant which is generally associated with the partial Fermi-level density of states (DOS) of the probed site,[34] and should be zero for the existence of a band gap at the Fermi level. Apparently, the small $1/T_{1K}T$ values indicate few but nonzero Fermi-level DOS for both materials. We thus classify the present CoTiSb samples as semimetals with finite DOS at the Fermi level. Such an argument is consistent with the result obtained from the single crystal, revealing a metallic ground state from the optical investigation.[35]

Above 150 K, $1/T_1T$ rises rapidly for both samples, with an activated temperature dependence. This is the characteristic behavior for semiconductors, with the enhancement in the relaxation rate arising from an increase in the number of carriers because of the thermal excitation across an energy gap. Bloembergen has calculated the relaxation rate in semiconductors due to conduction electrons as follows:[36]

$$\frac{1}{T_1} \propto \sqrt{T}n_e \propto T^2 e^{-E_g/2k_BT}. \quad (4)$$

The DOS in this case is assumed to be proportional to the square root of the energy near the band edge with the Fermi level at the midgap. The carrier density n_e of the conduction electrons varies with temperature according to $n_e \propto T^{3/2} \exp(-E_g/2k_BT)$.

Thus, it is easy to reconcile the metallic behavior observed at low temperatures with the high-T semiconducting character by assuming a two-band model where one band overlaps the Fermi level while the second band is separated by an energy gap, E_g. In this case, the relaxation rate is given by[36,37]

$$\frac{1}{T_1T} = \frac{1}{T_{1K}T} + ATe^{-E_g/2k_BT}. \quad (5)$$

Here, the prefactor A is associated with the effective mass of the carriers as well as their concentrations. Each $T_{1K}T$ value was obtained from the low-temperature result as mentioned above, and we found that Eq. (5) gives good agreement with the experimental data, shown as the dashed curves in Fig. 5. The values of E_g and A extracted from these fits are recorded in Table II. It is apparent that the energy gap of CoTiSb gradually increases from 0.15 to 0.19 eV upon annealing. Such a trend agrees well with the tendency of ΔE which is responsible for the reduction in the orbital Knight shift of the annealed sample.

The observed gap here is not actually a gap but rather a pseudogap with residual DOS around the Fermi level. This finding is consistent with the optical experiment which indicated CoTiSb to be a semimetal.[35] In order to address this quantitatively, we estimate the Fermi-level DOS from the Korringa constant. For the d-spin relaxation in metals, two relaxation mechanisms dominate the Korringa term: $1/T_{1K}T = (1/T_1T)_d + (1/T_1T)_{\text{orb}}$. The first part arises from the d-spin core polarization, while the second one is due to orbital electrons. Based on the noninteracting electron picture, $(1/T_1T)_d$ and $(1/T_1T)_{\text{orb}}$ can be expressed as[38]

$$\left(\frac{1}{T_1T}\right)_d = C[H_{hf}^d N_d(E_F)]^2 \left[\frac{1}{3}f^2 + \frac{1}{2}(1-f)^2\right]q, \quad (6)$$

TABLE II. Orbital Knight shift in %, prefactor A in units of 10^{-6} s^{-1} K^{-2}, gap size in eV, Korringa constant $1/T_{1K}T$ in units of 10^{-5} s^{-1} K^{-1}, and deduced Fermi-level d DOS in units of states/eV f.u. for each CoTiSb sample.

CoTiSb	K_{orb}	A	E_g	$1/T_{1K}T$	$N_d(E_F)$
As-cast	0.225	10	0.15	21	0.033
Annealed	0.217	8	0.19	7.6	0.020

$$\left(\frac{1}{T_1T}\right)_{orb} = C[H_{hf}^{orb}N_d(E_F)]^2\left[\frac{2}{3}f\left(2-\frac{5}{3}f\right)\right]q, \qquad (7)$$

with $C=2hk_B\gamma_n^2$. H_{hf}^d is the hyperfine field per electron of the Co d-electrons, H_{hf}^{orb} is the orbital hyperfine field per unit orbital angular momentum, and $N_d(E_F)$ is the partial Co d-electron DOS at the Fermi energy (E_F) in units of states/eV spin. The parameter f is the relative weight of the d orbitals in the t_{2g} states at the Fermi level,[39] and q is a factor equal to the reciprocal of the degeneracy.

As revealed from the band structure calculations on CoTiSb,[3,7] the wave functions around E_F are primarily of d character with t_{2g} symmetry, yielding the value of $f=1$. Furthermore, the cobalt d-electron manifold has three degeneracy in the reciprocal space near the Γ point, giving $q=1/3$. Taking $H_{hf}^d \sim -1.8 \times 10^5$ gauss and $H_{hf}^{orb} \sim 5.7 \times 10^5$ gauss in Co metals,[39,40] each $N_d(E_F)$ value can be obtained from the combination of Eqs. (6) and (7), with the results tabulated in Table II. The extracted partial Co-d Fermi-level DOS is quite small for each studied material, being consistent with the semimetallic characteristic for CoTiSb.[35]

The analysis of the spin-lattice relaxation rate clearly indicates that $N_d(E_F)$ is reduced by approximately 40% for our annealed CoTiSb sample as compared to the as-cast one. Such a change is found to be in good agreement with the variation in the electrical resistivity and the Seebeck coefficient.[13,14] In general, the decrease in the carrier concentration will cause a more semiconducting-like response where an increase in the magnitude of the electrical resistivity is commonly observed. For the Seebeck coefficient, it is basically true that a large Seebeck coefficient is brought about by a low $N_d(E_F)$.[41] Therefore, the previously observed enhancements in both electrical resistivity and Seebeck coefficient in the annealed CoTiSb alloys can be easily accounted for by the reduction in $N_d(E_F)$.

III. CONCLUSIONS

NMR measurements on the as-cast and annealed CoTiSb alloys have provided a concise picture for the changes in the local electronic properties. Clear evidence for the reduction of the Fermi-level DOS driven by heat treatment has been established. Since the annealing process has little effect on the Sb loss in CoTiSb, the association of the observed result with the Sb loss should be excluded. Rather, it can be attributed to the improvement of the structural perfection and thus the stronger hybridization between the p element and d metals. It turns out to be more semimetallic in the annealed CoTiSb sample which leads to enhancements in the electrical resistivity and the Seebeck coefficient as reported. We consider that the conclusions drawn from this comparative study are common features for the semiconducting and semimetallic half-Heusler compounds.

*cslue@mail.ncku.edu.tw

[1] M. A. Kouacou, J. Pierre, and R. V. Skolozdra, J. Phys.: Condens. Matter **7**, 7373 (1995).

[2] J. Pierre, R. V. Skolozdra, J. Tobola, S. Kaprzyk, C. Hordequin, M. A. Kouacou, I. Karla, R. Currat, and E. Lelievre-Berna, J. Alloys Compd. **262-263**, 101 (1997).

[3] J. Tobola, J. Pierre, S. Kaprzyk, R. V. Skolozdra, and M. A. Kouacou, J. Phys.: Condens. Matter **10**, 1013 (1998).

[4] F. G. Aliev, F. G. Brandt, V. V. Moshchalkov, V. V. Kozyrkov, R. V. Skolozdra, and A. I. Belogorov, Z. Phys. B **75**, 167 (1989).

[5] F. G. Aliev, V. V. Kozyrkov, V. V. Moshchalkov, R. V. Skolozdra, and K. Durczewski, Z. Phys. B **80**, 353 (1990).

[6] D. Young, P. Khalifah, R. J. Cava, and A. P. Ramirez, J. Appl. Phys. **87**, 317 (2000).

[7] B. R. K. Nanda and I. Dasgupta, J. Phys.: Condens. Matter **15**, 7307 (2003).

[8] H. Hohl, A. P. Ramirez, C. Goldman, G. Ernst, B. Wolfing, and E. Bucher, J. Phys.: Condens. Matter **10**, 7843 (1998).

[9] J. Tobola and J. Pierre, J. Alloys Compd. **296**, 243 (2000).

[10] C. Uher, J. Yang, S. Hu, D. T. Morelli, and G. P. Meisner, Phys. Rev. B **59**, 8615 (1999).

[11] Y. Xia, S. Bhattacharya, V. Ponnambalam, A. L. Pope, S. J. Poon, and T. M. Tritt, J. Appl. Phys. **88**, 1952 (2000).

[12] Y. Xia, V. Ponnambalam, S. Bhattacharya, A. L. Pope, S. J. Poon, and T. M. Tritt, J. Phys.: Condens. Matter **13**, 77 (2001).

[13] Yu. Stadnyk, Yu. Gorelenko, A. Tkachuk, A. Goryn, V. Davydov, and O. Bodak, J. Alloys Compd. **329**, 37 (2001).

[14] T. Sekimoto, K. Kurosaki, H. Muta, and S. Yamanaka, J. Alloys Compd. **394**, 122 (2005).

[15] B. Balke, G. H. Fecher, A. Gloskovskii, J. Barth, K. Kroth, C. Felser, R. Robert, and A. Weidenkaff, Phys. Rev. B **77**,

045209 (2008).

[16] T. Sekimoto, K. Kurosaki, H. Muta, and S. Yamanaka, Mater. Trans. **46**, 1481 (2005).

[17] T. Sekimoto, K. Kurosaki, H. Muta, and S. Yamanaka, Mater. Trans. **47**, 1445 (2006).

[18] C. S. Lue, B. X. Xie, and C. P. Fang, Phys. Rev. B **74**, 014505 (2006).

[19] C. S. Lue, S. M. Huang, C. N. Kuo, F. T. Huang, and M.-W. Chu, New J. Phys. **10**, 083029 (2008).

[20] *Metallic Shifts in NMR*, edited by G. C. Carter, L. H. Bennett, and D. J. Kahan (Pergamon, Oxford, 1977).

[21] M. Terada, K. Endo, Y. Fujita, T. Ohoyama, and R. Kimura, J. Phys. Soc. Jpn. **29**, 1091 (1970).

[22] M. Terada, K. Endo, Y. Fujita, and R. Kimura, J. Phys. Soc. Jpn. **32**, 91 (1972).

[23] C. P. Slichter, *Principles of Magnetic Resonance* (Springer-Verlag, New York, 1990).

[24] C. Kittel and Elihu Abrahams, Phys. Rev. **90**, 238 (1953).

[25] R. E. Walstedt and L. R. Walker, Phys. Rev. B **9**, 4857 (1974).

[26] C. S. Lue, Joseph H, Ross, Jr., K. D. D. Rathnayaka, D. G. Naugle, S. Y. Wu, and W.-H. Li, J. Phys.: Condens. Matter **13**, 1585 (2001).

[27] C. S. Lue, J. H. Ross, Jr., C. F. Chang, and H. D. Yang, Phys. Rev. B **60**, R13941 (1999).

[28] C. S. Lue, H. D. Yang, and Y. K. Kuo, Chin. J. Phys. **43**, 775 (2005).

[29] C.-S. Lue and Joseph H. Ross, Jr., Phys. Rev. B **58**, 9763 (1998).

[30] C. S. Lue and Joseph H. Ross, Jr., Phys. Rev. B **61**, 9863 (2000).

[31] C. S. Lue and S. C. Chen, Phys. Rev. B **79**, 125108 (2009).

[32] A. Narath, Phys. Rev. **162**, 320 (1967).

[33] Toru Moriya, *Spin Fluctuations in Itinerant Electron Magnetism* (Springer-Verlag, Berlin, 1985).

[34] J. Korringa, Physica **16**, 601 (1950).

[35] L. Degiorgi, A. V. Sologubenko, H. R. Ott, F. Drymiotis, and Z. Fisk, Phys. Rev. B **65**, 041101(R) (2001).

[36] N. Bloembergen, Physica **20**, 1130 (1954).

[37] Dieter Wolf, *Spin Temperature and Nuclear-Spin Relaxation in Matter* (Clarendon, Oxford, 1979).

[38] B. Nowak, Solid State Nucl. Magn. Reson. **21**, 53 (2002).

[39] G. N. Rao, Hyperfine Interact. **7**, 141 (1979).

[40] C. S. Lue, Y. T. Lin, and C. N. Kuo, Phys. Rev. B **75**, 075113 (2007).

[41] N. F. Mott and H. Jones, *The Theory of the Properties of Metals* (Clarendon, Oxford, 1936).